Self-Assembled Plasmonic Core–Shell Clusters with an Isotropic Magnetic Dipole Response in the Visible Range

Stefan Mühlig,[†,*] Alastair Cunningham,[‡] Sebastian Scheeler,[§,⊥] Claudia Pacholski,[§,⊥] Thomas Bürgi,[‡] Carsten Rockstuhl,[†] and Falk Lederer[†]

[†]Institute of Condensed Matter Theory and Solid State Optics, Abbe Center of Photonics, Friedrich-Schiller-Universität Jena, Max-Wien-Platz 1, 07743 Jena, Germany, [‡]Département de Chimie Physique, Université de Genève, Quai Ernest-Ansermet 30, 1211 Genève, Switzerland, [§]Max-Planck-Institut für Intelligente Systeme, Heisenbergstrasse 3, 70569 Stuttgart, Germany, and [⊥]Department of Biophysical Chemistry, University of Heidelberg, Im Neuenheimer Feld 253, 69120 Heidelberg, Germany

ABSTRACT We theoretically analyze, fabricate, and characterize a three-dimensional plasmonic nanostructure that exhibits a strong and isotropic magnetic response in the visible spectral domain. Using two different bottom-up approaches that rely on self-organization and colloidal nanochemistry, we fabricate clusters consisting of dielectric core spheres, which are smaller than the wavelength of the incident radiation and are decorated by a large number of metallic nanospheres. Hence, despite having a complicated inner geometry, such a core–shell particle is sufficiently small to be perceived as an individual object in the far field. The optical properties of such complex plasmonic core–shell particles are discussed for two different core diameters.

KEYWORDS: core–shell nanostructure · isotropic magnetic resonance · localized surface plasmon resonance · self-assembly · bottom-up technology · colloidal nanochemistry

Metallic nanoparticles and more complex composites thereof have been intensively investigated during the past century.[1] The excitation of localized surface plasmon polaritons at discrete wavelengths is usually the key feature that attracts the interest. As the terminology already suggests, these hybrid excitations are bound to the interface between a metal and a dielectric where an external electromagnetic illumination can resonantly drive the charge density oscillations in the metal. The resulting excitation carries its energy partially in the photonic and partially in the plasmonic state. The contribution of both can be tailored by suitably adjusting the nanoparticles' geometry, the near- or far-field coupling to adjacent objects, and/or the excitation conditions. Potentially, the most appealing property of such localized surface plasmon polaritons is their field concentration on the length scale of evanescent waves. This therefore allows the usual resolution limit predicted by far-field optics to be overcome. With a lifetime exceeding that of an optical cycle, a coherent buildup of the fields leads additionally to large near-field enhancements. Their exploitation is promising for many future nanoscopic applications since plasmonic effects can link the macroscopic to the nanoscopic word, and evidently *vice versa*.

A prominent class of applications exploits the field enhancement for biosensing with nanoparticles[2,3] or surface-enhanced Raman scattering using complex-shaped plasmonic structures.[4,5] Other applications are associated with the localized generation of heat due to dissipation in metallic nanoparticles.[6] This very localized plasmonic heat generation can be exploited in cancer therapy.[7] Apart from that, plasmonic structures can also be incorporated into solar cells to enhance the light absorption.[8,9] Analytical models, like the hybridization scheme[10] or transformation optics approaches,[11] have been used to describe the coupling among adjacent plasmonic nanostructures. This allows a deep physical understanding of fabricated structures and fostered the prediction of many effects based on novel complex plasmonic structures like asymmetric dimers,[12] quadrumers,[13] or oligomers.[14] In particular, Fano-like resonances were observed in these structures.[15]

However, most of the applications mentioned above rely on plasmonic resonances with an electric dipolar character. This is obviously only one side of the coin. Considering simple structures like two coupled plasmonic nanospheres (a dimer) and using the hybridization model, antisymmetric resonances were forecast where the excited electric dipoles in both spheres are oscillating 180° out of phase.[16] Such an eigenmode is strongly subradiant and will be perceived as a magnetic dipole in the far-field.

* Address correspondence to stefan.muehlig@uni-jena.de.

Received for review May 28, 2011 and accepted June 29, 2011.

Published online June 29, 2011
10.1021/nn201969h

This magnetic response is the key ingredient for many further applications. It is required, for example, for perfect imaging where the field from an object is reconstructed with unprecedented resolution in the image plane[17] or in the field of transformation optics where control over the anisotropic electric and magnetic response of the structure is crucial.[18]

Using classical top-down nanofabrication technologies, structures exhibiting a strong magnetic dipolar response have been fabricated.[19,20] However, they suffer from many limitations. For example, it is difficult to achieve fully bulk materials, which are, however, required for realistic applications. Moreover, the usual periodic arrangement of the plasmonic structures along with their mesoscopic size usually prevents an isotropic response. Recently, bottom-up technologies for the fabrication of structures were proposed where asymmetric resonances (that can be related to a magnetic dipole oscillation) can be excited and first results have been reported.[12,21,22] However, in most of these contributions, the self-assembled structures were situated in a planar fashion on a substrate. In this article, we advance the field by demonstrating two approaches for the fabrication of fully three-dimensional clusters in solution by means of colloidal nanochemistry that exhibit a strong isotropic magnetic response. These clusters consist of dielectric spheres, which are decorated by a large number of isolated, nontouching metallic nanospheres. Previously, this kind of structure has been proposed as a promising candidate for exhibiting artificial magnetism.[23,24] This magnetism can be explained by assuming that the shell of metallic nanospheres acts effectively as a medium with an extremely high permittivity at wavelengths slightly above the collective plasmonic resonance. The large permittivity in turn evokes Mie resonances. For the lowest order one, the electric displacement field rotates in a plane perpendicular to the polarization of the incident magnetic field. Therefore, this mode can be associated with the desired magnetic dipole contribution (a detailed discussion about this mode is given in the Supporting Information). Such an explanation applies not just for core–shell clusters but also for spherical aggregates of many metallic nanospheres.[25,26] Although a few publications on the fabrication of such core–shell systems exist,[27−33] their optical response was never related to the excitation of an isotropic magnetic dipole moment. Thus, it is the aim of this contribution to establish this relation. It has to be mentioned that magnetic dipoles can also be excited in dielectric spheres exhibiting a large real part of the permittivity.[34,35] In particular, spheres made of silicon have recently attracted a lot of attention.[36,37]

RESULTS AND DISCUSSION

To document the entire chain of research, in what follows, we investigate core–shell clusters fabricated by two distinct self-assembly processes. Both techniques rely on colloidal nanochemistry and exploit distinguishable bottom-up strategies to self-assemble the clusters. The first fabrication technique takes advantage of electrostatic forces between positively charged silica microspheres and negatively charged gold nanospheres. This technique has been already proven powerful for the fabrication of layered arrays of gold nanospheres.[38] The second self-assembly technique uses thiol chemistry to attach the gold nanospheres onto the silica spheres. The fabricated structures, moreover, differ in that they use dielectric spheres of different size, enabling an experimental study of scaling effects. We present measured extinction spectra of the fabricated samples and compare them to rigorous simulations. There, the nominal geometry of the core–shell clusters is fully taken into account by using an extended Mie theory to compute the scattering response of large aggregates of spheres. From such theoretical considerations, we can draw the conclusion that the measured resonance, which is strongly redshifted compared to that of an isolated gold nanosphere, can be related to a magnetic dipole moment.

To distinguish between both fabrication processes, from now on, we will term core–shell clusters fabricated by self-assembling due to electrostatic forces as "electrostatic assembly" and those fabricated due to thiol chemistry as "thiol assembly". In Figure 1, scanning electron micrographs (SEMs) of both structures are shown. They consist of silica spheres with a radii of 78 $\pm$ 6 nm (thiol assembly) and radii of 130 $\pm$ 10 nm (electrostatic assembly). These silica spheres are decorated by gold nanospheres with radii of 8 $\pm$ 1 nm and 10 $\pm$ 2 nm for thiol assembly and electrostatic assembly, respectively, leading to approximately 275 and 320 gold nanospheres covering the silica spheres. As can be seen from Figure 1, both self-assembling processes allow fabricating core–shell clusters with a sufficiently large number of gold nanospheres attached to the silica spheres. The first step of the optical characterization consists of the measurement of the extinction spectra of the fabricated core–shell clusters in solution. The solvent of thiol assembly is toluene and that of electrostatic assembly is dominated by water. The respective extinction measurements are presented in Figure 2. Note that all extinction curves are normalized to their respective maximum in the investigated spectral domain. As can be seen by the red solid curves in Figure 2, the localized plasmon polariton resonances of the single gold nanospheres occur at 530 and 521 nm for thiol assembly and electrostatic assembly, respectively, represented by maxima in the extinction spectra. The slightly different resonance frequency for both single nanospheres is due to the different permittivities of the solvents. The resonances of the core–shell clusters are displayed as blue dashed curves in Figure 2, where the extinction peaks at 600 nm for thiol assembly

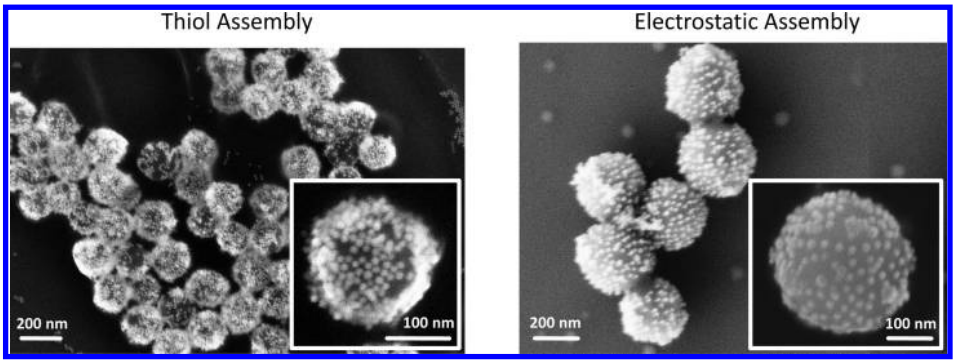

Figure 1. Scanning electron micrographs of fabricated core–shell clusters (for geometrical details, see text). An amorphous arrangement of core–shell clusters of thiol assembly and of electrostatic assembly is shown in the left and right panels, respectively. The inset of both micrographs depicts a zoomed in view showing a single core–shell cluster.

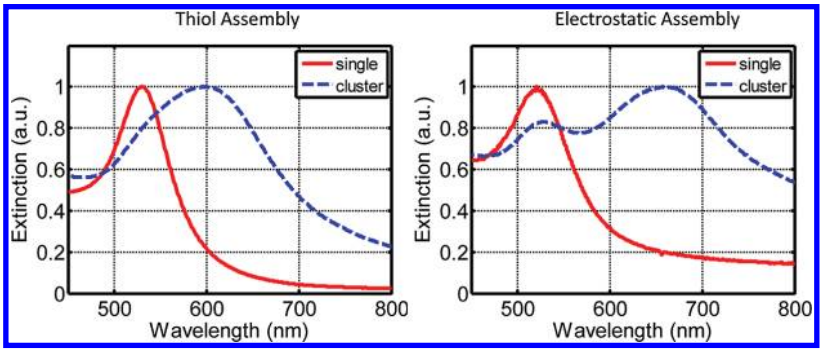

Figure 2. Measured extinction spectra of fabricated core–shell clusters (see Figure 1) in solution (blue dashed curve). For comparison, the extinction spectra of the single gold nanospheres are shown (red solid curve).

and at 670 nm for electrostatic assembly. These resonances are strongly red-shifted when compared to the resonance of the individual gold nanosphere. In the following, we are going to simulate the optical response of the fabricated structures. By using these results, the measured red-shifted peaks of the core–shell cluster extinction can be related to a magnetic dipolar response.

In this article, we apply the extended Mie theory[39,40] to simulate the optical response of the fabricated core–shell clusters. We consider single core–shell clusters with geometrical parameters fixed by the experimental conditions, take the fine details of a respective arrangement into account, and calculate the extinction cross sections of these structures. The results are shown in Figure 3. The respective cluster geometry (of the simulations) shown in the insets corresponds to the fabricated structures. The radius of the silica sphere was set to 80 nm, and it was covered by an amorphous arrangement of 274 gold nanospheres with radii of 8 nm for thiol assembly. The permittivity of the solvent toluene was assumed to be 2.24. The radius of the silica sphere in the simulations of electrostatic assembly was set to be 130 nm, and it was covered by an amorphous arrangement of 354 gold nanospheres with radii of 10 nm. The permittivity of the solvent water was set to be 1.77. Material parameters of gold were taken from literature[41] with a size-dependent correction of the imaginary part.[42] All series expansions in Mie theory were considered up to the fifth order, where the first order corresponds to a field expansion that considers electric and magnetic dipoles only. The core–shell clusters are illuminated by a plane wave. All curves in Figure 3 are equally normalized to their resonance peak in the investigated spectral domain.

The simulated extinction spectra (Figure 3) show an excellent agreement with the measurements (Figure 2). The red-shifted resonances of the core–shell clusters appear at 605 and 660 nm for thiol assembly and electrostatic assembly, respectively. These resonance positions match the experimental data almost perfectly. The slight deviation is caused by two facts. First, in simulations, only one single core–shell cluster is considered, whereas in experiments, an amorphous arrangement of clusters in solution is probed. Second, as indicated previously, the geometrical parameters of the fabricated samples could be only accounted for up to a certain precision. Because the peak position of the red-shifted resonance depends on these geometrical parameters, we identify this limited precision as the most likely reason for these marginal deviations. Of course, the simulation results could be adjusted by varying the geometrical parameters, but considering the almost perfect agreement, we refrain from doing so.

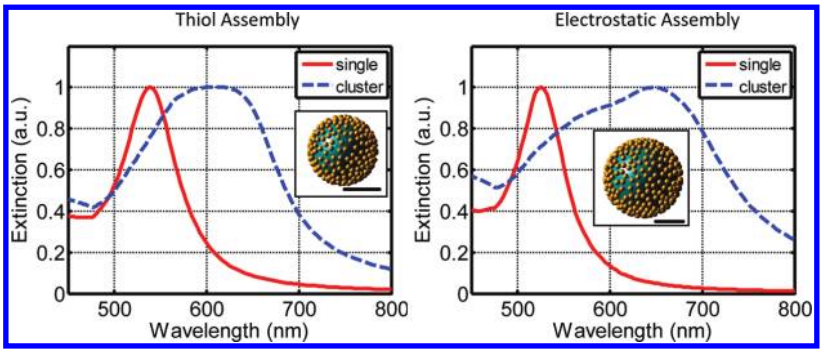

Figure 3. Simulated extinction spectra of core–shell clusters (see Figure 1) in solution (blue dashed curves). The insets show a sketch of the structures under investigation (for geometrical parameters, see text; the black scale bar corresponds to 100 nm in both structures). As for the measured spectra (see Figure 2), the extinction spectra of the single gold nanospheres are shown (red solid curves).

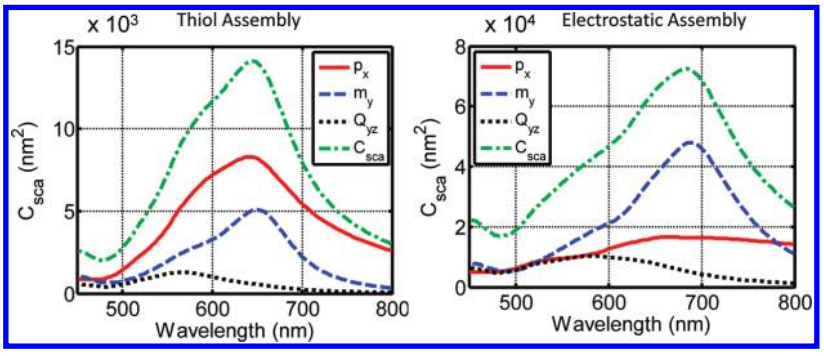

Figure 4. Simulated contributions of the relevant multipole moments (p, electric dipole; m, magnetic dipole; Q̂, electric quadrupole) to the scattering cross section of the core–shell clusters as a function of the wavelength.

One feature in the measured spectra of the core–shell cluster of electrostatic assembly is not reproduced by simulations. This concerns a second peak at the wavelength of the localized plasmon polariton resonance of single gold nanospheres (see Figure 2). In experiments, this peak is caused by gold nanospheres which do not cover the dielectric sphere but are left in solution because of the excess of gold nanospheres in the fabrication process. It is proposed that in the electrostatic assembly method an equilibrium exists between gold nanospheres in solution and at the surface of the silica cores. In this case, an excess of gold nanospheres would be required in order to ensure that the cores remain covered. As stated above, in the simulations, only a single core–shell cluster is considered whereas isolated gold nanospheres in solution are not taken into account. The absence of this effect for thiol assembly in the experimental spectra clearly demonstrates that almost all gold nanospheres cover the silica cores. Here the gold nanospheres are covalently bonded, and therefore, no excess of gold spheres is required in the fabrication process.

To identify extinction resonances with the excitation of a magnetic dipole moment in these structures, we investigate the contribution of the respective multipole moments to the scattered field of the core–shell clusters. This is easily done since in Mie theory all fields are represented by a series expansions corresponding to a multipole expansion in spherical coordinates. These spherical multipole moments can be transformed into Cartesian ones, which facilitates the identification of the conventional electric and magnetic multipoles. Details of such a multipole analysis for arbitrary-shaped scatterers can be found elsewhere.[43] The contribution of the most relevant multipole moments of both fabricated core–shell clusters to the scattered field of these structures is displayed in Figure 4. They are normalized such that their sum yields the complete scattering cross section. Higher order multipoles, not shown in Figure 4, provide only a negligible contribution. In the simulations, it is assumed that the core–shell clusters are illuminated by a linear polarized plane wave (similar to Figure 3) propagating in the *z* direction and polarized in the *x* direction, hence the components of the multipole moments are designated accordingly. The orientation of the coordinate system is, however, arbitrary because the structure exhibits spherical symmetry. From Figure 4, it can be clearly seen that the red-shifted resonance of the scattering cross section of the core–shell clusters is caused by a resonant magnetic dipole moment. This magnetic dipole dominates the spectrum for electrostatic assembly, and its strength compares to that of the electric dipole for thiol assembly. The differences between both assemblies can be related to the

different core diameters; that is, increasing the diameter leads to a more pronounced magnetic dipole compared to the electric one. Similar effects have been already reported in the literature.[26] We also observe a weak quadrupole contribution in both samples. However, this quadrupole resonance affects only slightly the scattering cross section, and it peaks at smaller wavelengths compared to the magnetic dipole resonance. The effect of this quadrupole moment is an increased absorption of the core–shell cluster near its resonance. This explains the different peak positions of the scattering (Figure 4) and the extinction cross section (Figure 3) in simulations. The increased absorption due to the excited quadrupole moment shifts the maximum of the extinction cross section to shorter wavelengths compared to the scattering cross section.

CONCLUSION

Two distinct fabrication processes are proposed and implemented based on chemical self-assembly for the fabrication of core–shell clusters consisting of silica cores which are decorated by a huge number of gold nanospheres. The measured extinction spectra are compared to rigorous simulations of the fabricated samples. Furthermore, by decomposing the scattered field into contributing multipole moments, we revealed a resonant isotropic magnetic dipole moment in the visible range. This magnetic resonance could be directly related to the measured red-shifted peak of the extinction spectra. The key result is the fabrication of a nanostructured material that exhibits artificial isotropic magnetism in the visible spectral domain.

METHODS

Core–Shell Clusters *via* Electrostatic Forces. The first self-assembly technique used electrostatic forces to attach the gold nanospheres onto the silica spheres. In a first step, the gold nanospheres were prepared according to the well-known Turkevich method.[44] In brief, 600 mL of a 0.25 mM solution of $HAuCl_4$ was heated to 100 °C under constant magnetic stirring. The gold was then reduced by the addition of 15 mL of a 0.03 M sodium citrate solution. Succeeding color changes were observed before a deep red solution arose, and after 15 min, the reaction vessel was removed from the heat and allowed to cool to room temperature.

Uniform silica microspheres with a mean diameter of 260 nm were purchased from Bangs Laboratories, Inc. In order to adsorb gold nanospheres at these silica microspheres, it was first necessary to alter the surface chemistry of the silica microspheres to induce an affinity between both constituents. This was achieved by taking advantage of silica chemistry[45] where the careful choice of reagents allows access to a wide variety of surface chemistries. In this case, *N*-[3-(trimethoxysilyl)propyl]-ethylenediamine was selected because of the terminal amine group, which presents a net positive charge and therefore an electrostatic attraction to the gold nanospheres, which are negatively charged as a result of the citrate capping molecules. Then 0.5 mL of the microspheres was added to 2 mL of a 5% (v/v) solution of *N*-[3-(trimethoxysilyl)propyl]ethylenediamine in ethanol and mixed under magnetic stirring for 30 min. Excess organosilane was removed by centrifuging the solution at 2000 rcf for 10 min before removing the supernatant and redispersing the now functionalized silica microspheres in 2 mL of ethanol.

To produce core–shell clusters, 10 μL of the functionalized silica core sphere solution was added to 40 mL of gold nanospheres solution under vigorous stirring. The adsorption of the gold nanospheres was instantaneous and caused a color change in transmission from red to deep blue. Partial purification was possible by a further centrifugation step (1000 rcf, 5 min), although it was evident that this did not result in complete removal of excess gold nanospheres. Unless otherwise stated, all chemicals were purchased from Sigma-Aldrich.

Core–Shell Clusters *via* Thiol Assembly. The second self-assembly technique used thiol chemistry to attach the gold nanospheres onto the silica spheres. The applied materials included the following: (3-mercaptopropyl)trimethoxysilane (MPS, Sigma-Aldrich) purified by distillation under reduced pressure, tetrachloroauric(III) acid ($HAuCl_4$, Sigma-Aldrich), and oleylamine (Acros Organics) used without further purification. Amicon Ultra 15 mL 100 k (Millipore) tubes were used for ultrafiltration.

Thiol group functionalized silica spheres were prepared according to an already published method by Nakamura and Ishimura.[46] In order to achieve monodisperse silica particles with a diameter of approximately 150 nm, 380 μL MPS was injected into 150 mL of ammonia solution (1%) at 50 °C under vigorous stirring. The reaction solution was vigorously stirred for 2 h. Afterward, the particles were separated by centrifugation and washed three times with 60 mL of ethanol. Further purification was obtained by ultrafiltration, and the purified particles were finally dispersed in 5 mL of toluene.

Gold nanospheres were synthesized using the method reported by Hiramatsu and Osterloh.[47] A solution of 300 mg of $HAuCl_4$, 4.9 g of oleylamine, and 5 mL of toluene was injected into a boiling solution of 8.5 g of oleylamine in 250 mL of toluene. The heat source was removed after 1 h. The gold nanospheres were precipitated with methanol, separated by centrifugation, and redispersed in toluene. Monodisperse fractions of the gold nanospheres were prepared by size-selective precipitation. Each fraction was dispersed in 5 mL of toluene. Gold nanosphere coated silica spheres were fabricated by adding 3 mL of gold nanosphere solution to 5 mL of silica particle solution, and the gold nanospheres were assembled on the silica particle surfaces, forming the core–shell clusters.[32] The observed color in transmission of the solution changed from red to blue within 15 min.

Mie Theory. The scattering of electromagnetic fields at spherical particles can be calculated by using Mie theory,[48] which is a rigorous solution of Maxwell's equations. In Mie theory, all fields are expanded into an infinite series of vector spherical harmonics, being the eigenfunctions of the problem, with unknown complex amplitudes. By applying the usual boundary conditions at the surface of the spheres, these amplitudes can be determined for any given incident field in a self-consistent manner. The framework of Mie theory for a single sphere can be extended toward clusters of arbitrarily arranged spheres.[39,40]

Acknowledgment. Financial support from the Federal Ministry of Education and Research (PhoNa), the State of Thuringia within the ProExcellence program (MeMa), the European Union (NANOGOLD) as well as the Max-Planck Society is acknowledged. The authors are grateful to C. Menzel for useful discussions.

Supporting Information Available: A detailed discussion about the excited magnetic dipole moment of the investigated core–shell clusters is given. Field distributions are presented as well as the influence of the dielectric core to the magnetic

resonance is disclosed. This material is available free of charge *via* the Internet at http://pubs.acs.org.

REFERENCES AND NOTES

1. Halas, N. J. Plasmonics: An Emerging Field Fostered by Nano Letters. *Nano Lett.* **2010**, *10*, 3816–3822.
2. McPhillips, J.; Murphy, A.; Jonsson, M. P.; Hendren, W. R.; Atkinson, R.; Hook, F.; Zayats, A. V.; Pollard, R. J. High-Performance Biosensing Using Arrays of Plasmonic Nanotubes. *ACS Nano* **2010**, *4*, 2210–2216.
3. Kabashin, A. V.; Evans, P.; Pastkovsky, S.; Hendren, W.; Wurtz, G. A.; Atkinson, R.; Pollard, R.; Podolskiy, V. A.; Zayats, A. V. Plasmonic Nanorod Metamaterials for Biosensing. *Nat. Mater.* **2009**, *8*, 867–871.
4. Li, J. F.; Huang, Y. F.; Ding, Y.; Yang, Z. L.; Li, S. B.; Zhou, X. S.; Fan, F. R.; Zhang, W.; Zhou, Z. Y.; Wu, D. Y.; *et al.* Shell-Isolated Nanoparticle-Enhanced Raman Spectroscopy. *Nature* **2010**, *464*, 392–395.
5. Taylor, R. W.; Lee, T.-C.; Scherman, O. A.; Esteban, R.; Aizpurua, J.; Huang, F. M.; Baumberg, J. J.; Mahajan, S. Precise Subnanometer Plasmonic Junctions for SERS within Gold Nanoparticle Assemblies Using Cucurbit[*n*]uril "Glue". *ACS Nano* **2011**, *5*, 3878–3887.
6. Baffou, G.; Quidant, R.; Garciá de Abajo, F. J. Nanoscale Control of Optical Heating in Complex Plasmonic Systems. *ACS Nano* **2010**, *4*, 709–716.
7. Loo, C.; Lowery, A.; Halas, N.; West, J.; Drezek, R. Immunotargeted Nanoshells for Integrated Cancer Imaging and Therapy. *Nano Lett.* **2005**, *5*, 709–711.
8. Ferry, V. E.; Sweatlock, L. A.; Pacifici, D.; Atwater, H. A. Plasmonic Nanostructure Design for Efficient Light Coupling into Solar Cells. *Nano Lett.* **2008**, *8*, 4391–4397.
9. Rockstuhl, C.; Lederer, F. Photon Management by Metallic Nanodiscs in Thin Film Solar Cells. *Appl. Phys. Lett.* **2009**, *94*, 213102.
10. Nordlander, P.; Oubre, C.; Prodan, E.; Li, K.; Stockman, M. I. Plasmon Hybridization in Nanoparticle Dimers. *Nano Lett.* **2004**, *4*, 899–903.
11. Aubry, A.; Lei, D. Y.; Maier, S. A.; Pendry, J. B. Plasmonic Hybridization between Nanowires and a Metallic Surface: A Transformation Optics Approach. *ACS Nano* **2011**, *5*, 3293–3308.
12. Brown, L. V.; Sobhani, H.; Lassiter, J. B.; Nordlander, P.; Halas, N. J. Heterodimers: Plasmonic Properties of Mismatched Nanoparticle Pairs. *ACS Nano* **2010**, *4*, 819–832.
13. Fan, J. A.; Bao, K.; Wu, C.; Bao, J.; Bardhan, R.; Halas, N. J.; Manoharan, V. N.; Shvets, G.; Nordlander, P.; Capasso, F. Fano-like Interference in Self-Assembled Plasmonic Quadrumer Clusters. *Nano Lett.* **2010**, *10*, 4680–4685.
14. Hentschel, M.; Dregely, D.; Vogelgesang, R.; Giessen, H.; Liu, N. Plasmonic Oligomers: The Role of Individual Particles in Collective Behavior. *ACS Nano* **2011**, *5*, 2042–2050.
15. Luk'yanchuk, B.; Zheludev, N. I.; Maier, S. A.; Halas, N. J.; Nordlander, P.; Giessen, H.; Chong, C. T. The Fano Resonance in Plasmonic Nanostructures and Metamaterials. *Nat. Mater.* **2010**, *9*, 707–715.
16. Riikonen, S.; Romero, I.; Garca de Abajo, F. J. Plasmon Tunability in Metallodielectric Metamaterials. *Phys. Rev. B* **2005**, *71*, 235104.
17. Pendry, J. B. Negative Refraction Makes a Perfect Lens. *Phys. Rev. Lett.* **2000**, *85*, 3966–3969.
18. Leonhardt, U.; Philbin, T. G. *Transformation Optics and the Geometry of Light*; Elsevier: Amsterdam, 2009; Vol. 53, Chapter 2, pp 69–152.
19. Enkrich, C.; Wegener, M.; Linden, S.; Burger, S.; Zschiedrich, L.; Schmidt, F.; Zhou, J. F.; Koschny, T.; Soukoulis, C. M. Magnetic Metamaterials at Telecommunication and Visible Frequencies. *Phys. Rev. Lett.* **2005**, *95*, 203901.
20. Valentine, J.; Zhang, S.; Zentgraf, T.; Ulin-Avila, E.; Genov, D. A.; Bartal, G.; Zhang, X. Three-Dimensional Optical Metamaterial with a Negative Refractive Index. *Nature* **2008**, *455*, 376–379.
21. Fan, J. A.; Wu, C.; Bao, K.; Bao, J.; Bardhan, R.; Halas, N. J.; Manoharan, V. N.; Nordlander, P.; Shvets, G.; Capasso, F. Self-Assembled Plasmonic Nanoparticle Clusters. *Science* **2010**, *328*, 1135–1138.
22. Grzelczak, M.; Vermant, J.; Furst, E. M.; Liz-Marzán, L. M. Directed Self-Assembly of Nanoparticles. *ACS Nano* **2010**, *4*, 3591–3605.
23. Simovski, C. R.; Tretyakov, S. A. Model of Isotropic Resonant Magnetism in the Visible Range Based on Core−Shell Clusters. *Phys. Rev. B* **2009**, *79*, 045111.
24. Vallecchi, A.; Albani, M.; Capolino, F. Collective Electric and Magnetic Plasmonic Resonances in Spherical Nanoclusters. *Opt. Express* **2011**, *19*, 2754–2772.
25. Rockstuhl, C.; Lederer, F.; Etrich, C.; Pertsch, T.; Scharf, T. Design of an Artificial Three-Dimensional Composite Metamaterial with Magnetic Resonances in the Visible Range of the Electromagnetic Spectrum. *Phys. Rev. Lett.* **2007**, *99*, 017401.
26. Mühlig, S.; Rockstuhl, C.; Yannopapas, V.; Bürgi, T.; Shalkevich, N.; Lederer, F. Optical Properties of a Fabricated Self-Assembled Bottom-Up Bulk Metamaterial. *Opt. Express* **2011**, *19*, 9607–9616.
27. Caruso, F.; Spasova, M.; Saigueirino-Maceira, V.; Liz-Marzán, L. M. Multilayer Assemblies of Silica-Encapsulated Gold Nanoparticles on Decomposable Colloid Templates. *Adv. Mater.* **2001**, *13*, 1090–1094.
28. Gittins, D. I.; Susha, A. S.; Schoeler, B.; Caruso, F. Dense Nanoparticulate Thin Films *via* Gold Nanoparticle Self-Assembly. *Adv. Mater.* **2002**, *14*, 508–512.
29. Sadtler, B.; Wei, A. Spherical Ensembles of Gold Nanoparticles on Silica: Electrostatic and Size Effects. *Chem. Commun.* **2002**, *15*, 1604–1605.
30. Salgueiriño-Maceira, V.; Caruso, F.; Liz-Marzán, L. M. Coated Colloids with Tailored Optical Properties. *J. Phys. Chem. B* **2003**, *107*, 10990–10994.
31. Pastoriza-Santos, I.; Gomez, D.; Perez-Juste, J.; Liz-Marzán, L. M.; Mulvaney, P. Optical Properties of Metal Nanoparticle Coated Silica Spheres: A Simple Effective Medium Approach. *Phys. Chem. Chem. Phys.* **2004**, *6*, 5056–5060.
32. Lu, Z.; Goebl, J.; Ge, J.; Yin, Y. Self-Assembly and Tunable Plasmonic Property of Gold Nanoparticles on Mercapto-Silica Microspheres. *J. Mater. Chem.* **2009**, *19*, 4597.
33. Xue, J.; Wang, C.; Ma, Z. A Facile Method To Prepare a Series of SiO_2@Au Core/Shell Structured Nanoparticles. *Mater. Chem. Phys.* **2007**, *105*, 419–425.
34. Wheeler, M. S.; Aitchison, J. S.; Mojahedi, M. Three-Dimensional Array of Dielectric Spheres with an Isotropic Negative Permeability at Infrared Frequencies. *Phys. Rev. B* **2005**, *72*, 193103.
35. Seo, B.-J.; Ueda, T.; Itoh, T.; Fetterman, H. Isotropic Left Handed Material at Optical Frequency with Dielectric Spheres Embedded in Negative Permittivity Medium. *Appl. Phys. Lett.* **2006**, *88*, 161122.
36. Evlyukhin, A. B.; Reinhardt, C.; Seidel, A.; Luk'Yanchuk, B. S.; Chichkov, B. N. Optical Response Features of Si-Nanoparticle Arrays. *Phys. Rev. B* **2010**, *82*, 045404.
37. Garca-Etxarri, A.; Gómez-Medina, R.; Froufe-Pérez, L. S.; López, C.; Chantada, L.; Scheffold, F.; Aizpurua, J.; Nieto-Vesperinas, M.; Sáenz, J. J. Strong Magnetic Response of Submicron Silicon Particles in the Infrared. *Opt. Express* **2011**, *19*, 4815–4826.
38. Cunningham, A.; Mühlig, S.; Rockstuhl, C.; Bürgi, T. Coupling of Plasmon Resonances in Tunable Layered Arrays of Gold Nanoparticles. *J. Phys. Chem. C* **2011**, *115*, 8955–8960.
39. Xu, Y.-L. Electromagnetic Scattering by an Aggregate of Spheres. *Appl. Opt.* **1995**, *34*, 4573–4588.
40. Mühlig, S.; Rockstuhl, C.; Pniewski, J.; Simovski, C. R.; Tretyakov, S. A.; Lederer, F. Three-Dimensional Metamaterial Nanotips. *Phys. Rev. B* **2010**, *81*, 075317.
41. Johnson, P. B.; Christy, R. W. Optical Constants of the Noble Metals. *Phys. Rev. B* **1972**, *6*, 4370–4379.
42. Okamoto, T. Near-Field Spectral Analysis of Metallic Beads. In *Near-Field Optics and Surface Plasmon Polaritons*; Kawata, S., Ed.; Springer: Berlin, 2001; Vol. 81, pp 97–123.
43. Mühlig, S.; Menzel, C.; Rockstuhl, C.; Lederer, F. Multipole Analysis of Meta-Atoms. *Metamaterials* **2011**in press.

44. Kimling, J.; Maier, M.; Okenve, B.; Kotaidis, V.; Ballot, H.; Plech, A. Turkevich Method for Gold Nanoparticle Synthesis Revisited. *J. Phys. Chem. B* **2006**, *110*, 15700–15707.
45. Iler, R. K. *The Chemistry of Silica—Solubility, Polymerization, Colloid and Surface Properties, and Biochemistry*; Wiley: New York, 1979.
46. Nakamura, M.; Ishimura, K. Synthesis and Characterization of Organosilica Nanoparticles Prepared from 3-Mercaptopropyltrimethoxysilane as the Single Silica Source. *J. Phys. Chem. C* **2007**, *111*, 18892–18898.
47. Hiramatsu, H.; Osterloh, F. E. A Simple Large-Scale Synthesis of Nearly Monodisperse Gold and Silver Nanoparticles with Adjustable Sizes and with Exchangeable Surfactants. *Chem. Mater.* **2004**, *16*, 2509–2511.
48. Bohren, C. F.; Huffman, D. R. *Absorption and Scattering of Light by Small Particles*; Wiley: New York, 1979.